Food Chemistry 334 (2021) 127487

Contents lists available at ScienceDirect

Food Chemistry

journal homepage: www.elsevier.com/locate/foodchem

Optimizing interfacial adhesion in PBAT/PLA nanocomposite for biodegradable packaging films

Shuo Qiu[a], Yikai Zhou[a], Geoffrey I.N. Waterhouse[a,b], Ruizhi Gong[a], Jiazhuo Xie[a], Kun Zhang[a], Jing Xu[a,*]

[a] College of Chemistry and Material Science, Shandong Agricultural University, Tai'an 271018, PR China
[b] School of Chemical Sciences, The University of Auckland, Auckland 1142, New Zealand

ARTICLE INFO

Keywords:
PBAT
PLA
POSS
Compatibility
Biodegradable packaging film

ABSTRACT

Biodegradable films poly(butylene adipate-*co*-butylene terephthalate) (PBAT)/poly(lactic acid) (PLA) incorporated with nano-polyhedral oligomeric silsesquioxane ($POSS_{(epoxy)8}$) as a reactive compatibilizer were developed by melt processing. Structural, morphological, mechanical, and gas permeability properties of the films were determined. ^{1}H NMR and GPC demonstrated that the $POSS_{(epoxy)8}$ was chemically bound at the PBAT/PLA boundary phase via an epoxide ring opening reaction. SEM micrographs of impact fracture surfaces demonstrated the $POSS_{(epoxy)8}$ improved interfacial adhesion between PBAT and PLA matrix. The mechanical properties of the PBAT/PLA films containing $POSS_{(epoxy)8}$ were enhanced relative to pristine PBAT/PLA films. The water vapor, CO_2 and O_2 permeability of the PBAT/PLA films were improved by $POSS_{(epoxy)8}$ addition. PBAT/PLA films containing $POSS_{(epoxy)8}$ were shown to be superior to pristine PBAT/PLA films and polyethylene films in food storage tests. Results suggest that $POSS_{(epoxy)8}$ addition during PBAT/PLA film production offers a simple strategy for the production of high performance biodegradable plastic packaging films.

1. Introduction

Reducing the amount of plastic packaging films entering landfills and the environment is a global challenge, demanding changes in the way we manufacture plastics and how we use and recycle plastics. One of the best strategies for minimizing plastic packaging films is to manufacture biodegradable plastics. These plastics, after a certain period of time or exposure to certain stimuli (e.g. moisture, UV light, biological micro-organisms, etc), are decomposed to simple chemicals which ideally are naturally occurring molecules and non-toxic. Poly (butylene adipate-*co*-butylene terephthalate) (PBAT) is a fully biodegradable aromatic copolyester with good ductility, and a potential alternative to polyolefin-based packaging materials (Pan, Ai, Shao, Chen, & Gao, 2019; Wu et al, 2019). However, the high melt viscosity, low crystallization rate, low tensile strength, and high cost currently restrict its processability and industrial applications. To overcome these drawbacks, PBAT is typically blended with other biopolymers to make high performance composite materials.

Amongst the different biopolymers that can be blended with PBAT, poly(lactic acid) (PLA) is a very promising candidate due to its desirable properties such as high stiffness, reasonable strength, as well as relatively low cost (Jin, Hu, & Park, 2019). However, producing high performance PBAT/PLA melt blend products is technically challenging, since the two polymers are not particularly compatible. Their incompatibility and immiscibility result in PBAT/PLA composites with poor tensile properties, preventing their use in applications where composites might be subjected to mechanical stress. The large difference in the solubility parameters between PBAT and PLA leads to weak interfacial adhesion between the constituent in pristine PBAT/PLA melt blends (Correa, Bacigalupe, Maggi, & Eisenberg, 2016). Improving the performance of PBAT/PLA composites relies on the discovery of suitable compatibilizers which can improve interfacial adhesion between PBAT and PLA during melt blending.

A wide range of compatibilizers and compatibilization approaches have been trialed in an attempt to improve the properties of PBAT/PLA composites. Plasticizing and chain extension/branching in the molten state can improve interfacial bonding between PLA and PBAT (Coltelli, Toncelli, Ciardelli, & Bronco, 2011). Various compatibilizers and additives have been shown to improve the interface compatibility and deliver composites and products with improved performance relative to pristine PBAT/PLA blends. Amongst these, multi-functional epoxy compounds (i.e. small organic molecules or oligomers) have been

* Corresponding author.
E-mail address: jiaxu@sdau.edu.cn (J. Xu).

https://doi.org/10.1016/j.foodchem.2020.127487
Received 9 April 2020; Received in revised form 10 June 2020; Accepted 1 July 2020
Available online 07 July 2020

applied extensively as chain extenders for PLA/PBAT blends during reactive extrusion (Dong, Zou, Yan, Ma, & Chen, 2013). In this case, the epoxy functional groups react with nucleophilic end groups on the PLA and PBAT chains (i.e. −OH and −COOH groups, respectively) to extend chain lengths, resulting in composites with high ductility. However, these organic compounds can have a detrimental effect on the glass transition temperature (T_g) and tensile properties of PBAT/PLA blends. To overcome these shortcomings, an inorganic agent can also be introduced as a reinforcing filler to improve the mechanical properties of PBAT/PLA composites. Instead of adding both a chain extender and fillers in PBAT/PLA composite melt blending, a prudent synthetic strategy would be identifying a new compatibilizer that has both reactive groups (i.e. epoxy, for chain extension) and can impart rigidity (to improve the tensile properties of the resulting composite). Such a multifunctional additive would greatly simplify the synthesis of high performance PBAT/PLA melt blended composites.

$POSS_{(epoxy)8}$ represents a very promising additive for improving the compatibility of PBAT/PLA blends, consisting of an inorganic silsesquioxane cage as the core with eight attached glycidyl groups (Fig. S1). $POSS_{(epoxy)8}$ is often used as adhesive and reinforcing material in coatings on glass surfaces to enhance the scratch and mark resistance (Waddon, Zheng, Farris, & Coughlin, 2002). Recently, it has been successfully applied as a compatibilizer and carrier in coatings and resins (Iacono, Budy, Mabry, & Smith, 2007; Nakamura, & Naka, 2013; Chinnam, & Wunder, 2011; Yang et al, 2014; Arshad, Kaur, & Ullah, 2016; Zhang, Zhang, & Guan, 2015; Li et al, 2017; Tanaka, Ishiguro, & Chujo, 2010; Gardella, Basso, Prato, & Monticelli, 2013; Wu, Bhattacharya, & Morgan, 2013). In these applications, the inorganic core composed of a silicon-oxygen framework binds with polymer molecules to inhibit their chain motion, thereby improving the thermal stability and mechanical properties of the polymers (Abdelwahab, Misra, & Mohanty, 2015; Konnola, Nair, & Joseph, 2015; Ko, Hong, Park, Gupta, Choi, & Bhattacharya, 2009; Al-Itry, Lamnawar, & Maazouz, 2014a,b). In addition, the epoxy groups on $POSS_{(epoxy)8}$ can undergo in-situ ring-opening reactions with the reactive end groups on the polymer chains, making it a near ideal compatibilizer for melt blending PBAT and PLA. To date, the compatibilization of PBAT/PLA blends with $POSS_{(epoxy)8}$ has received little attention, motivating a detailed investigation.

In the present study, we aimed to improve the properties of PBAT/PLA nanocomposite films prepared by twin-screw melt extrusion followed by melt blowing process, by including $POSS_{(epoxy)8}$ at loadings in the range 0.5–5 wt%. The structure and morphology of these resulting films were then investigated in detail using ^{1}H NMR, GPC, XRD and SEM. The thermal, mechanical and gas permeation properties of the resulting PBAT/PLA composites were also explored. From this work, we aimed to evaluate the merit of $POSS_{(epoxy)8}$ as a functional additive and compatibilizer in PBAT/PLA melt blends and films, and also to identify the optimal $POSS_{(epoxy)8}$ loading.

2. Materials and methods

2.1. Materials

PBAT (Grade: 8003f) with an average molecular weight of 141,000 g mol^{-1} was supplied by Hangzhou Xinfu Pharmaceutical Co, Ltd., China. PLA (Grade: 4032D) with an average molecular weight of 253,000 g mol^{-1} and a dispersion index of 2.28 was purchased from Nature Works. $POSS_{(epoxy)8}$ (Grade: EP0409, 1.5 nm diameter) in viscous liquid form was obtained from Hybrid Plastics Company, USA. $POSS_{(epoxy)8}$ has an inorganic silsesquioxane cage core and eight organic glycidyl groups attached at the corners of the cage, as shown in Fig. S1.

2.2. Preparation of PBAT/PLA/POSS(epoxy)$_8$ composites

The PBAT and PLA polymers were first dried at 85 °C under vacuum for 12 h to prevent hydrolytic degradation and pinhole defect formation during melt blending. The melt blending process used a discontinuous twin screw extruder with a screw length to diameter (L/D) ratio of 40. Polymeric material (1000 g, PBAT/PLA 85/15 by weight, with or without $POSS_{(epoxy)8}$) was fed into the metering section of the extruder which had seven successive temperature zones: 160 °C, 175 °C, 190 °C, 190 °C, 190 °C, 175 °C, and 165 °C. The polymer feed rate was set as 150 g min^{-1} with the rotors operating a speed of 60 rpm to achieve a stable melt flow and to avoid thermal degradation of PLA. The concentration of $POSS_{(epoxy)8}$ in the final nanocomposites was adjusted to be 0, 0.5, 1, 3 or 5 wt%.

2.3. Preparation of PBAT/PLA/POSS(epoxy)$_8$ films

PBAT/PLA/POSS(epoxy)$_8$ films with a thickness of 60–70 μm were prepared in a single screw extrusion blow molding machine FB-300 (see Fig. S2). The diameter screw was 20 mm with length-to-diameter (L/D) ratio of 25. An annular die of 40 mm diameter, with die gap of 0.80 mm, was used to shape the initial tube dimensions. The processing temperature across the different heating zones of the blow molding machine ranged from 170 to 190 °C. The screw speed in the film extruder was 26 rpm, with a speed of 2.4 m min^{-1}. The PBAT/PLA/$POSS_{(epoxy)8}$ composite films produced are denoted herein as POSS-x (where × is the wt.% of $POSS_{(epoxy)8}$). For instance, POSS-0.5 represents the film containing 0.5 wt% $POSS_{(epoxy)8}$. A pristine PBAT/PLA film (POSS-0) was fabricated via the same process without $POSS_{(epoxy)8}$ addition.

2.4. Proton nuclear magnetic resonance spectroscopy (^{1}H NMR)

^{1}H nuclear magnetic resonance spectroscopy was used to analyze the degree of epoxy group reaction when $POSS_{(epoxy)8}$ was incorporated into the PBAT/PLA/$POSS_{(epoxy)8}$ films. Films were dissolved in deuterated chloroform ($CDCl_3$) and tetramethylsilane (TMS) was added as the internal chemical shift standard. ^{1}H NMR spectra were collected on Mercury Plus-400 spectrometer (Varian).

2.5. Gel permeation chromatography (GPC)

The weight-average molecular weights (M_w) for the pristine PBAT/PLA and PBAT/PLA/$POSS_{(epoxy)8}$ films were measured using a GPC system (Waters 515 HPLC Pump, Waters 2414 detector). Polystyrene standards with different average molecular weights were used to generate the calibration curve. The GPC tests were conducted using $HCCl_3$ as the solvent and eluent.

2.6. X-ray diffraction (XRD)

X-ray powder diffraction (XRD) patterns were collected on a Bruker D8 ADVANCE X-ray diffractometer equipped with a Ni-filtered Cu K_α radiation source (40 kV, 40 mA).

2.7. Scanning electron microscopy (SEM)

The fracture surface morphologies of the PBAT/PLA/$POSS_{(epoxy)8}$ films and the dispersion of the $POSS_{(epoxy)8}$ in the films were investigated using scanning electron microscopy (Merlin Compact, Germany). Films were freeze fractured in liquid nitrogen, then gold-coated to reduce specimen charging during analyses. Silicon mapping analyses to identify POSS nanoparticles were performed using energy dispersive X-ray (EDX) spectroscopy. The electron beam energy was 3.00 KV for EDX measurements.

2.8. Tensile and tear test

Test specimens were cut from the PBAT/PLA/$POSS_{(epoxy)8}$ films and kept in a dessicator at room temperature for 24 h before the tests. The tensile and tear properties of the specimens were conducted using an UTM2502 testing machine equipped with a 500 N load cell. Crosshead speeds of 500 mm min^{-1} and 200 mm min^{-1} were used for the tensile and tear tests, respectively (according to GB/T 1040.3-2006). For each sample, at least five replicate specimens were subjected to mechanical testing, with the average of these tests being reported herein.

2.9. Water vapor transmission rate (WVTR)

The water vapor transmission characteristics of the films were analyzed using a Labthink W3/031 automatic water vapor transmission tester according to the ASTM E 96 test method. The experimental temperature was 38 °C and the relative humidity was 90%. The continuous mode was selected for the tests. Three specimens of each film were measured and the average value reported.

2.10. Gas permeability test

The oxygen transmission rate (OTR) and carbon dioxide transmission rate (CTR) of the PBAT/PLA and PBAT/PLA/$POSS_{(epoxy)8}$ films, as well as a LDPE film, were measured in duplicate at 25 °C using a manometric gas permeability tester (VAC-V1; Labthink, Shandong, China) employing the ASTM 1434–82 standard. Gas permeability measurements were performed using a constant-volume method at a feed pressure of 1 atm and a feed temperature of 20 °C. The diameter and thickness of the samples were 100 mm and 70 μm, respectively.

2.11. Sample packaging and storage

Strawberries, bananas and mushrooms were obtained from a local supermarket in Tai'an, China. Produce free of any obvious physical damage were separately heat-sealed packaged in prepared bags with dimensions of 15 × 10 cm and stored in the dark at room temperature for 11 days. The appearance and freshness of the produce were recorded after 11 days storage. As a control, strawberry, banana and mushroom without packaging were also stored in the dark for 11 days.

3. Results and discussion

3.1. ^1H NMR and GPC

^1H NMR and GPC were employed to characterize the chemical composition and structure of $POSS_{(epoxy)8}$, pristine PBAT/PLA film, and the PBAT/PLA/$POSS_{(epoxy)8}$ films. To confirm that the epoxy groups of $POSS_{(epoxy)8}$ reacted during melt processing of PBAT/PLA/$POSS_{(epoxy)8}$, ^1H NMR analyses were performed on PBAT/PLA (POSS-0) and PBAT/PLA/$POSS_{(epoxy)8}$ (POSS-5) films. A comparison of the ^1H NMR spectra of $POSS_{(epoxy)8}$, POSS-0, and POSS-5 (Fig. S3A–C) revealed distinct differences between the samples. $POSS_{(epoxy)8}$ has eight epoxy groups, with the protons in the epoxy groups accounting for 2.19 wt% of the molecule. The characteristic epoxy protons of $POSS_{(epoxy)8}$ appear 3.18–3.09 ppm in the ^1H NMR spectrum (Fig. S3A). For POSS-5 (containing 5 wt% $POSS_{(epoxy)8}$), some epoxy peaks can also be seen, along with the characteristic peaks of PBAT and PLA (as expected, the epoxy signals were absent in the ^1H NMR spectrum of POSS-0). By ratioing the peak area for epoxy protons against the area of all the proton signals for the POSS-5 film, and converting to mass ratios (Fu, Wang, Zhao, Horiuchi, & Li, 2017), we estimated that the residual amount of $POSS_{(epoxy)8}$ with intact epoxy groups to be ~0.05 wt%, a very small amount of the total amount of $POSS_{(epoxy)8}$ added in the POSS-5 sample (5 wt%). It can therefore be concluded that almost all the epoxy groups in the $POSS_{(epoxy)8}$ had reacted via ring opening during melt processing of the PBAT/PLA/$POSS_{(epoxy)8}$ films.

To further prove that $POSS_{(epoxy)8}$ was chemically integrated into the PBAT/PLA films, the weight-average molecular weight (M_W) of the POSS-0, POSS-0.5 and POSS-5 films were measured by GPC. As seen in Fig. S4, the average molecular weight of the PBAT/PLA/$POSS_{(epoxy)8}$ films increased with increasing $POSS_{(epoxy)8}$ content. The POSS-5 films had an average molecular weight that was 23,937 g mol^{-1} higher than that of POSS-0 films (an increase of about 19%). This indicates that reactions between $POSS_{(epoxy)8}$ and the PBAT or PLA polymers in the films resulted in the formation of longer polymeric chains. Since $POSS_{(epoxy)8}$ has eight reactive end groups, several PBAT or PLA chains could be chemically bounded to one POSS molecule, resulting in the development of chain extended or branched or cross-linked structures. Importantly, all the PBAT/PLA/$POSS_{(epoxy)8}$ films could be completely dissolved in chloroform, thus the extent of branching reactions involving $POSS_{(epoxy)8}$ were not so extensive that they resulted in heavy cross-linking or gel formation. This result is in good general agreement with the findings of Al-Itry et al., 2012, Al-Itry, Lamnawar, & Maazouz, 2014a,b.

3.2. XRD and SEM analysis

XRD and SEM analyses were employed to investigate the structure, morphology and interfacial properties of the PBAT and PLA components in the films. Fig. S5 shows normalized XRD patterns for PBAT/PLA/$POSS_{(epoxy)8}$ films containing different content amounts of $POSS_{(epoxy)8}$. Since the main matrix for all the films was PBAT, the XRD patterns for the films were dominated by the characteristic diffraction peaks of PBAT at 16.3, 17.6, 20.5, 23.1 and 25.0°, corresponding to the (011), (010), (110), (100) and (111) planes, respectively. The relative intensities of the XRD peaks associated with PBAT changed as the content of $POSS_{(epoxy)8}$ in the films increased, possibly due to preferential orientation effects or lattice strain introduced via polymer chain crystallization around the $POSS_{(epoxy)8}$ compatibilizer (Khan, Asiri, & Alamry, 2015). No new reflections appeared in the XRD patterns of PBAT/PLA/$POSS_{(epoxy)8}$ films relative to the POSS-0 reference, which indicated the incorporation of $POSS_{(epoxy)8}$ nanoparticles did not affect the crystalline phase of the polymer matrix.

SEM micrographs of PBAT/PLA films, with and without $POSS_{(epoxy)8}$, along the longitudinal impact fracture surface are shown in Fig. 1A. In the absence of $POSS_{(epoxy)8}$, the interfacial adhesion between PBAT and PLA was poor, as indicated by the abundance of non-bound PLA fibers and the void spaces throughout the fracture surface of the film (marked with white arrows in the POSS-0 SEM image). Adding $POSS_{(epoxy)8}$ even at low levels (0.1 wt%) greatly improved the interfacial adhesion between the PBAT and PLA, with the PLA in composites not debonding from the matrix. When the content of $POSS_{(epoxy)8}$ reached 1 wt%, there is no obvious phase separation between PBAT and PLA. It is clear that in the high magnification SEM images of Fig. 1A, the interfacial interactions in the PBAT/PLA/$POSS_{(epoxy)8}$ films improved in the presence of POSS particles, with the fibrous PLA being well-embedded and bonded within the PBAT matrix.

The transverse fracture surfaces of the POSS-0 and POSS-1 films were also studied to obtain further information about the interfacial interactions in these films (Fig. 1B). The fracture surface of POSS-0 was smooth, showing some islands and ovoid cavities resulting from the PLA being pulled out of the PBAT matrix. Incorporation of 1 wt% $POSS_{(epoxy)8}$ improved the compatibility. Some longer PLA nanofibrils/bars have been pulled out of the PBAT matrix during the fracturing, though these fibers have an adhering layer on their surface (indicated by white arrows). This is consistent with $POSS_{(epoxy)8}$ acting as a compatibilizer and chain extender, creating PBAT-co-POSS-co-PLA composite interfaces.

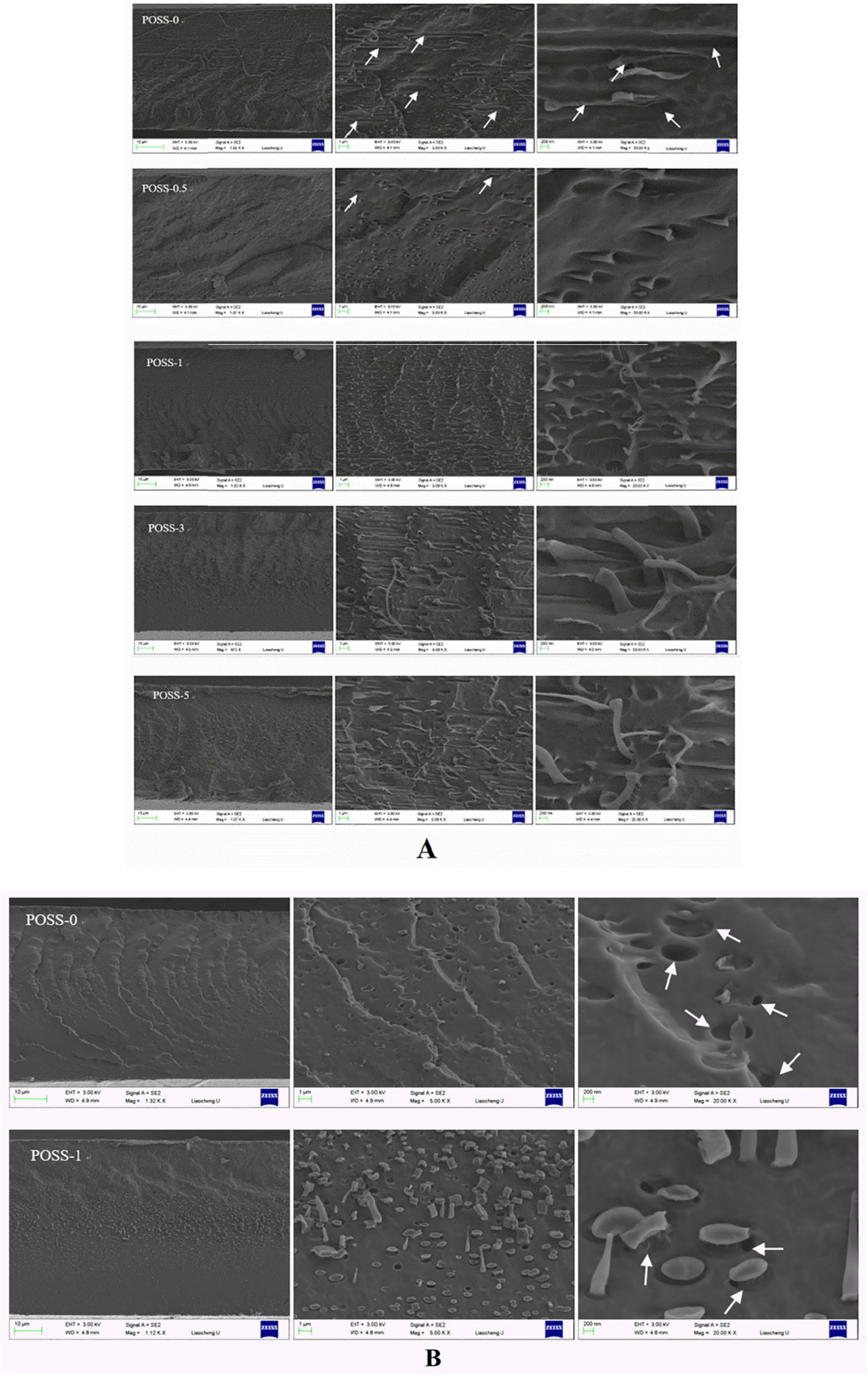

Fig. 1. SEM images of (A) the longitudinal fracture surface of POSS-0, POSS-0.5, POSS-1, POSS-3, POSS-5; (B) the transverse fracture surface of POSS-0 and POSS-1.

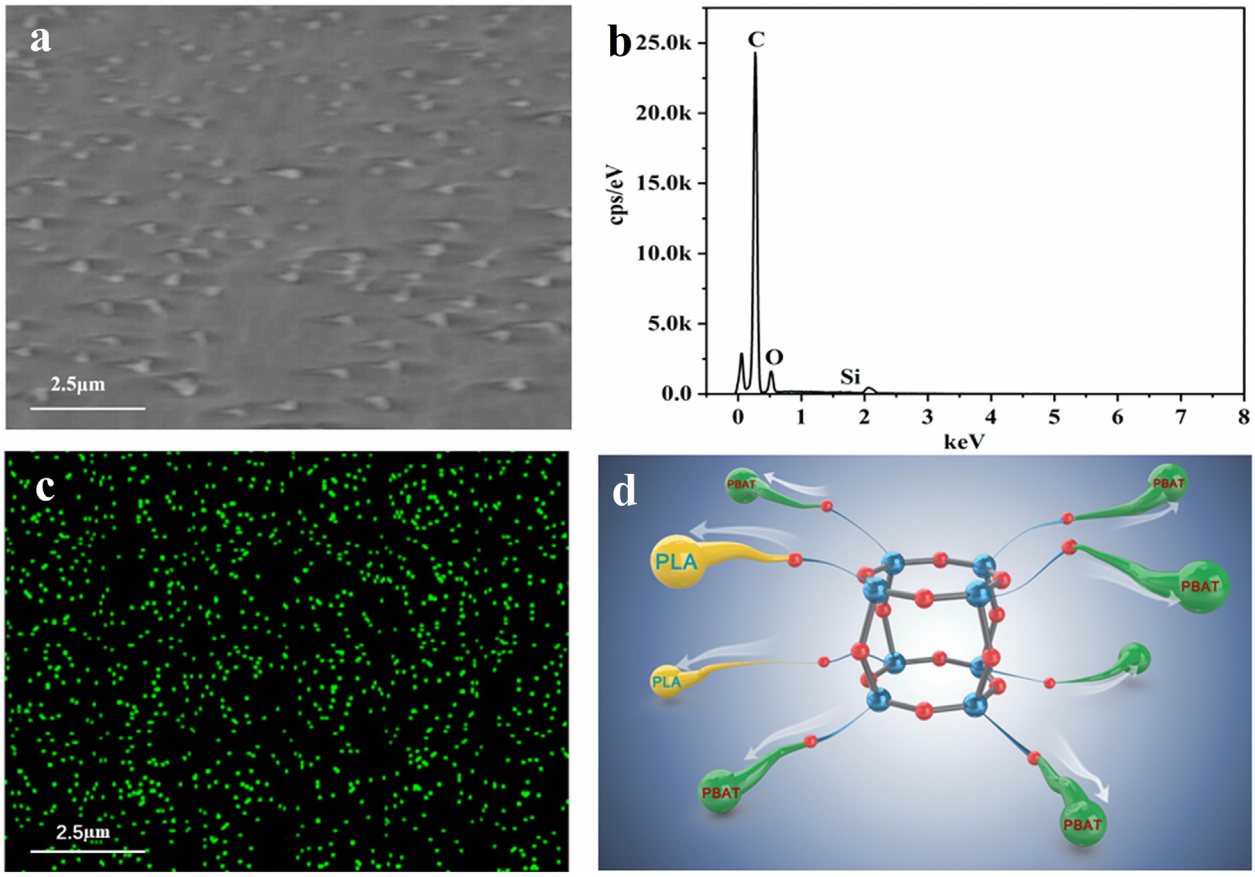

Fig. 2. (a) SEM image, (b) EDX spectrum and (c) EDX maps for POSS-1, and (d) schematic representation of the interface interaction between PLA and PBAT.

3.3. Energy dispersive X-ray (EDX) analysis

To further understand the dispersion and localization of $POSS_{(epoxy)8}$ particles in the polymer matrix, energy dispersive X-ray (EDX) analyses were performed on POSS-1 films. The green spots in the Si K X-ray maps in the transversal cross section of film (Fig. 2c) show the presence of silicon. The EDX map shows a uniform distribution of silicon, confirming a very good dispersion of POSS nanoparticles within polymer matrix, including the PBAT-PLA interface and PBAT matrix (Fig. 2c). Results suggest that the POSS nanoparticles link PBAT and PLA chains, as shown in Fig. 2d.

3.4. Mechanical behavior

The longitudinal and transverse tensile and tear strengths of the different PBAT/PLA/$POSS_{(epoxy)8}$ films were shown in Fig. 3. The addition of POSS dramatically increased the mechanical performance of the PBAT/PLA films in both directions. The results suggest that the uniform dispersion and strong interface interaction of POSS in the polymer films confers both a reinforcing and plasticizing effect, thus increasing the tensile strength and toughness of PBAT/PLA/$POSS_{(epoxy)8}$ films. A $POSS_{(epoxy)8}$ content of 1 wt% gave films with the optimum tensile strength, tear strength and longitudinal elongation at break, as well as the smallest difference between values in the transverse and longitudinal directions (see Fig. 3).

3.5. Water vapor transmission rate (WVTR) and gas permeability

The gas permeability of packaging films is vital to the postharvest shelf life of fresh produce. Accordingly, the oxygen, carbon dioxide, and water vapor permeability of POSS-0, POSS-1, POSS-5 and low-density polyethylene (LDPE) films with the same thickness were evaluated. The PBAT/PLA based films possessed high water vapor permeability than the LDPE film (Fig. 4A), consistent with PBAT having a high water permeability (Xie et al., 2018; Li, Lai, Wu, Severtson, & Wang, 2018). Further, $POSS_{(epoxy)8}$ addition increased the WVTR of PBAT/PLA films markedly (WVTR enhancements were 45 and 71% for POSS-1 and POSS-5, respectively, relative to POSS-0).

Gas permeabilities for the PBAT/PLA/$POSS_{(epoxy)8}$ films followed the order $P(CO_2) > P(O_2)$, which was expected based on the gas kinetic diameters (CO_2 3.3 Å; O_2 3.46 Å). This permeability results from the interplay between gas diffusivity and also the solubility of gas molecules in the polymer matrix (Kinoshita et al., 2017). As the $POSS_{(epoxy)8}$ loading increased, the permeability of all gasses increased dramatically whilst the selectivity remained similar to that of the neat POSS-0 film. The permeability coefficients for the films reflect the increase in the fractional free volume caused by the introduction of bulky porous POSS cages within the films (Dasgupta, Sen, & Banerjee, 2010). This change in gas permeability with POSS addition is depicted schematically in Fig. 5. The high permeability, without significant changes in selectivity, can be attributed to the non-selective passage of the gas molecules along the interfaces between the POSS particle and PBAT/PLA polymer host.

Fruit and vegetables degrade easily due to their high moisture content. Strawberries, bananas and mushrooms are especially perishable due to their relatively high metabolic activity. They typically have short ripening and senescent periods that make distribution and supply to consumers challenging. Based on the results of water vapor transmission tests, it was anticipated that the PBAT/PLA/$POSS_{(epoxy)8}$ films should be near ideal packaging materials for these moisture sensitive produce, avoiding anoxic conditions and the condensation of water vapor inside packaging bags. Further, the atmosphere inside packaging also influences produce shelf life, with the gas permeability of

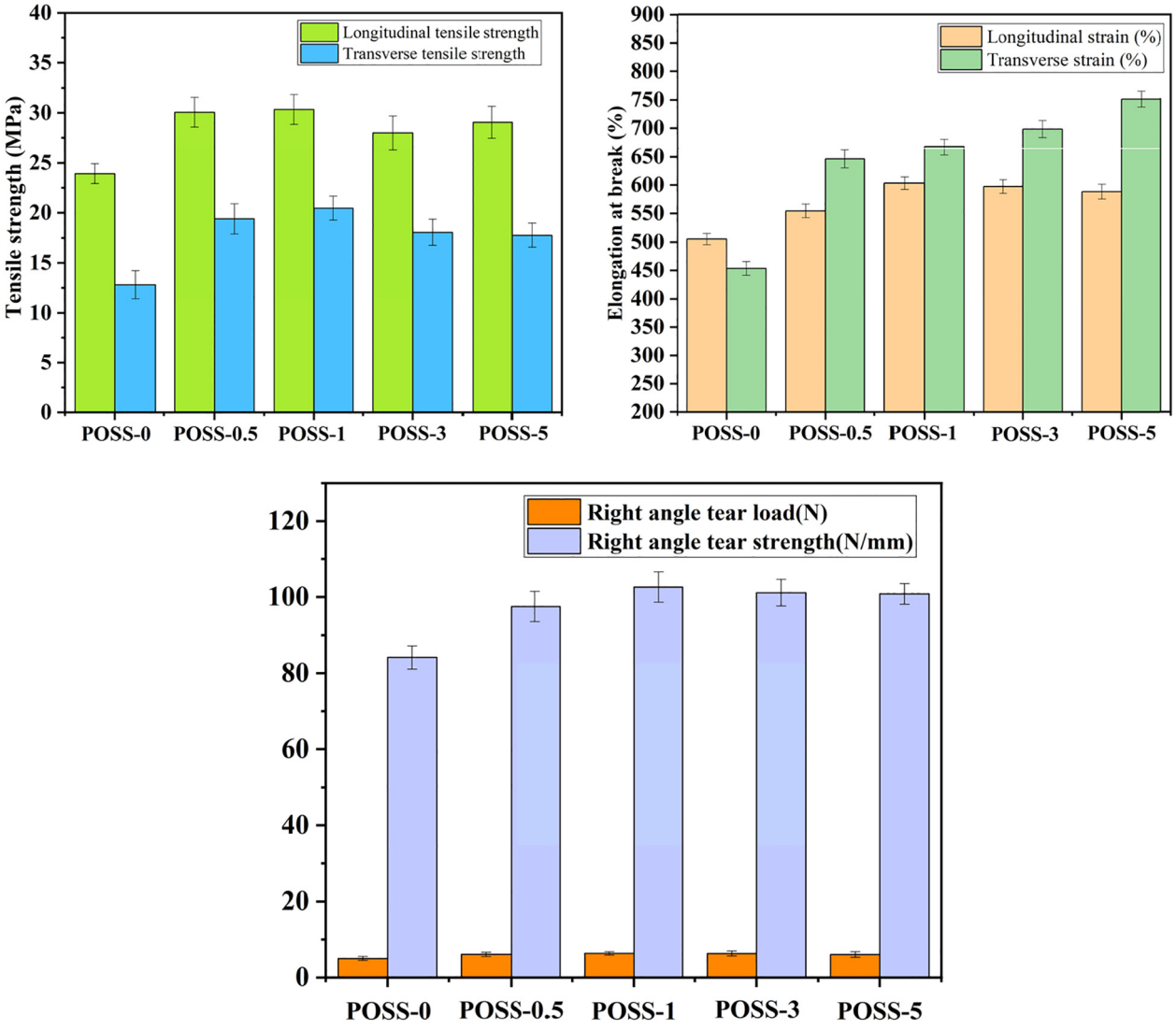

Fig. 3. Mechanical properties of PBAT/PLA films containing different amounts of $POSS_{(epoxy)8}$.

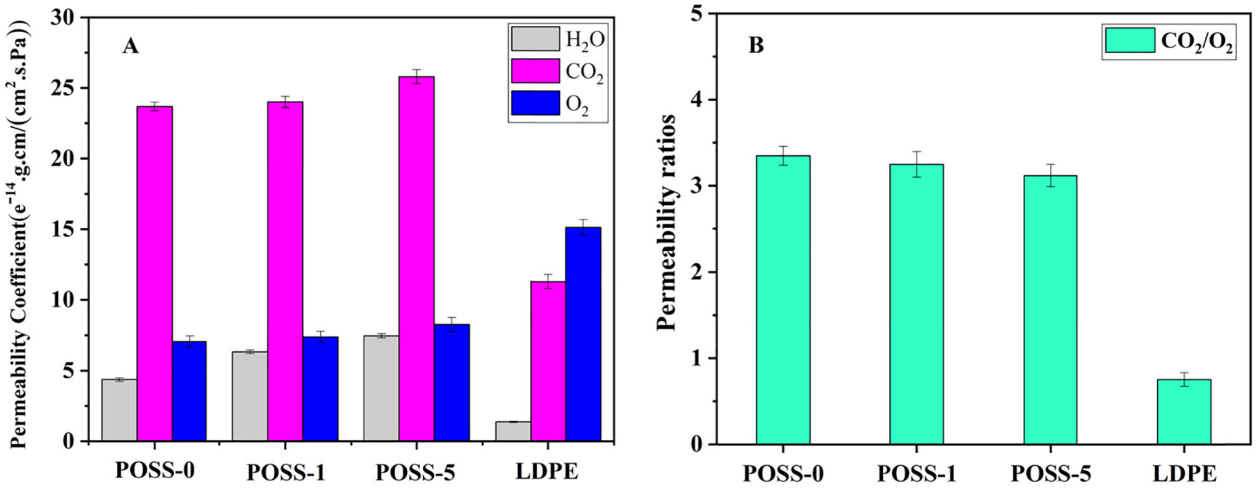

Fig. 4. Water, CO_2 and O_2 transmission rates (A) and permeability ratios of the CO_2 to O_2 of POSS-0, POSS-1, POSS-5, and LDPE films (B).

packaging material being important for regulating the respiration rate of fruits and vegetable. Respiration produces CO_2 and consume the O_2 in the microenvironment of package. On account of relative gas pressure differences between the inside and outside of the package, CO_2 will be released to the atmosphere and O_2 will enter the package (assuming that the film is both CO_2 and O_2 permeable). Thus, plastic films

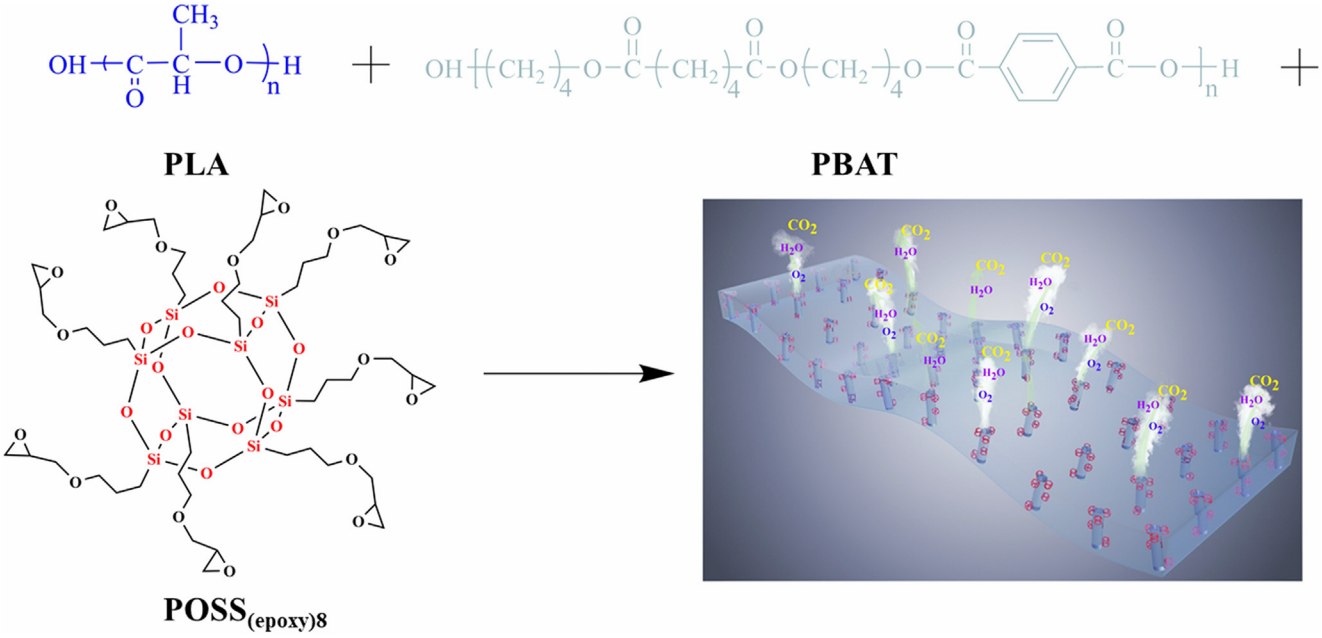

Fig. 5. Schematic diagram of gas permeation in PBAT/PLA/$POSS_{(epoxy)8}$ films.

with appropriate permeability to O_2, CO_2 and water vapor can significantly prolong the shelf-life of fruit and vegetables (Yun et al, 2017). For food packaging applications, the permselectivity (β = P(CO_2)/P(O_2)) and P(CO_2) are important factors for selecting suitable packaging material, especially for fresh fruits and vegetables. If the β value and P(CO_2) are small, the gas exchange will be very slow, thus giving potentially anoxic conditions and/or undesirably high CO_2 concentrations in the packaging head space (Turan, Sängerlaub, Stramm, & Gunes, 2017). As seen in Fig. 4B, PBAT/PLA/$POSS_{(epoxy)8}$ films had a higher β and P(CO_2) than LDPE. Therefore, the high permselectivity of the PBAT/PLA/$POSS_{(epoxy)8}$ films will prevent CO_2 accumulation and it can be used for the packaging of CO_2-sensitive produce and commodities.

3.6. Sample packaging and storage

To explore the potential application of the PBAT/PLA/$POSS_{(epoxy)8}$ films in fresh food packaging, we stored mushrooms, strawberries and bananas in sealed bags made using the polymer films. Controls experiments were also conducted using no packaging, POSS-0 films and LDPE films.

To allow direct visual comparison studies to be performed on the strawberries, bananas and mushrooms, the produce was removed from the bags they had been stored in after 11 days. Fig. 6 shows that produce stored without packaging or in the LDPE bags showed serious weight loss and was moldy respectively. Conversely, produce stored in the PBAT/PLA (POSS-0), POSS-1 and POSS-5 bags remained in good condition. Clearly, the good water vapor permeability of PBAT-based composite films kept the produce in a low moisture environment, which suppressed the growth of fungi (Li et al, 2019). In the case of banana, the POSS-0 and LDPE bags had a slight smell of ethanol when opened, suggesting some sugar fermentation had occurred. Fig. 6 also shows the cross section of bananas stored under the different conditions. The flesh near the skin had obvious deterioration in the case of bananas stored in the LDPE and POSS-0 bags, presumably through anaerobic respiration and the condensation. In the case of the bananas stored in the POSS-1 and POSS-5 bags, the banana skin had thinned appreciably due to moisture loss but the flesh remained in good condition. Strawberries and mushrooms packaged in POSS-1 and POSS-5 bags showed good color after 11 days storage. The results of the produce storage trial suggest that biodegradable PBAT/PLA/$POSS_{(epoxy)8}$ films have great potential as packaging materials for highly perishable, high-value fruits and vegetables. Importantly, the permeability of H_2O, CO_2 and O_2 in the packaging films can be tuned simply by varying the $POSS_{(epoxy)8}$ content, thus allowing respiration rates to be adjusted to the appropriate level for optimal preservation. These results encourage the widespread application of biodegradable PBAT/PLA/$POSS_{(epoxy)8}$ films in food packaging.

4. Conclusions

In conclusion, we have successful prepared biodegradable PBAT/PLA nanocomposite films containing a polyhedral oligomeric oilsesquioxane ($POSS_{(epoxy)8}$, loadings 0.5–5 wt%) via melt reactive extrusion followed by melt blowing. ^{1}H NMR and GPC verified that the epoxy functional groups of $POSS_{(epoxy)8}$ reacted covalently with the end groups PBAT and PLA, thereby greatly improving the interfacial adhesion between PBAT and PLA. The degree of crystallinity of the PBAT matrix was enhanced by $POSS_{(epoxy)8}$ addition. The mechanical properties of the PBAT/PLA/$POSS_{(epoxy)8}$ nanocomposite films, including tensile strength, elongation at break and tear strength all improved dramatically with $POSS_{(epoxy)8}$ addition, with 1 wt% $POSS_{(epoxy)8}$ being optimal. The incorporation of the porous $POSS_{(epoxy)8}$ cages in the PBAT/PLA films also enhanced the permeability of water vapor, CO_2 and O_2. Fruit and mushroom produce storage tests confirmed that PBAT/PLA/$POSS_{(epoxy)8}$ nanocomposite films outperformed pristine PBAT/PLA films and commercial LDPE packing films. Results suggest that $POSS_{(epoxy)8}$ addition greatly enhances the physical properties and performance of biodegradable PBAT/PLA films for food packaging applications.

CRediT authorship contribution statement

Shuo Qiu: Conceptualization, Writing - original draft, Methodology, Investigation. **Yikai Zhou:** Software, Validation. **Geoffrey I.N. Waterhouse:** Visualization. **Ruizhi Gong:** Supervision. **Jiazhuo Xie:** Formal analysis. **Kun Zhang:** Resources. **Jing Xu:** Methodology, Writing - review & editing, Funding acquisition.

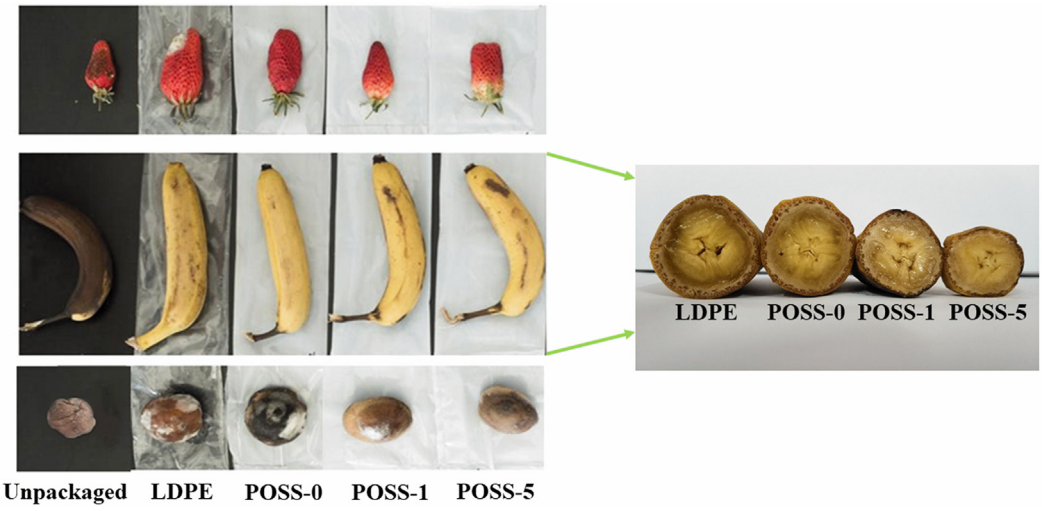

Fig. 6. Photographs of strawberries, bananas and mushrooms stored in air and in different types of plastic bags for 11 days. The image on the right shows the cross sections of the bananas stored in the different types of plastic bag.

Declaration of Competing Interest

The authors declare that they have no known competing financial interests or personal relationships that could have appeared to influence the work reported in this paper.

Acknowledgements

This work was supported by the National Key R&D Plan (No. 2016YFB0302400), and Agricultural Key Applied Technology Innovation Project of Shandong Province (2017, No. 6). GINW acknowledges funding support from the MacDiarmid Institute for Advanced Materials and Nanotechnology.

Appendix A. Supplementary data

Supplementary data to this article can be found online at https://doi.org/10.1016/j.foodchem.2020.127487.

References

Abdelwahab, M. A., Misra, M., & Mohanty, A. K. (2015). Epoxidized pine oil-siloxane: Crosslinking kinetic study and thermomechanical properties. *Journal of Applied Polymer Science, 132*.

Al-Itry, R., Lamnawar, K., & Maazouz, A. (2012). Improvement of thermal stability, rheological and mechanical properties of PLA, PBAT and their blends by reactive extrusion with functionalized epoxy. *Polymer Degradation and Stability, 97*, 1898–1914.

Al-Itry, R., Lamnawar, K., & Maazouz, A. (2014a). Reactive extrusion of PLA, PBAT with a multi-functional epoxide: Physico-chemical and rheological properties. *European Polymer Journal, 58*, 90–102.

Al-Itry, R., Lamnawar, K., & Maazouz, A. (2014b). Rheological, morphological, and interfacial properties of compatibilized PLA/PBAT blends. *Rheologica Acta, 53*, 501–517.

Arshad, M., Kaur, M., & Ullah, A. (2016). Green biocomposites from nanoengineered hybrid natural fiber and biopolymer. *ACS Sustainable Chemistry & Engineering, 4*(3), 1785–1793.

Chinnam, P. R., & Wunder, S. L. (2011). Polyoctahedral silsesquioxane-nanoparticle electrolytes for lithium batteries: POSS-lithium salts and POSS-PEGs. *Chemistry of Materials, 23*, 5111–5121.

Coltelli, M.-B., Toncelli, C., Ciardelli, F., & Bronco, S. (2011). Compatible blends of biorelated polyesters through catalytic transesterification in the melt. *Polymer Degradation and Stability, 96*, 982–990.

Correa, J. P., Bacigalupe, A., Maggi, J., & Eisenberg, P. (2016). Biodegradable PLA/PBAT/clay nanocomposites: Morphological, rheological and thermomechanical behavior. *Journal of Renewable Materials, 4*, 258–265.

Dasgupta, B., Sen, S. K., & Banerjee, S. (2010). Aminoethylaminopropylisobutyl POSS-Polyimide nanocomposite membranes and their gas transport properties. *Materials Science and Engineering, B, 168*, 30–35.

Dong, W., Zou, B., Yan, Y., Ma, P., & Chen, M. (2013). Effect of chain-extenders on the properties and hydrolytic degradation behavior of the poly(lactide)/poly(butylene adipate-co-terephthalate) blends. *International Journal of Molecular Sciences, 14*, 20189–20203.

Fu, Z., Wang, H., Zhao, X., Horiuchi, S., & Li, Y. (2017). Immiscible polymer blends compatibilized with reactive hybrid nanoparticles: Morphologies and properties. *Polymer, 132*, 353–361.

Gardella, L., Basso, A., Prato, M., & Monticelli, O. (2013). PLA/POSS nanofibers: A novel system for the immobilization of metal nanoparticles. *ACS Applied Materials & Interfaces, 5*, 7688–7692.

Iacono, S. T., Budy, S. M., Mabry, J. M., & Smith, D. W. (2007). Synthesis, characterization, and surface morphology of pendant polyhedral oligomeric silsesquioxane perfluorocyclobutyl aryl ether copolymers. *Macromolecules, 40*, 9517–9522.

Jin, F.-L., Hu, R.-R., & Park, S.-J. (2019). Improvement of thermal behaviors of biodegradable poly(lactic acid) polymer: A review. *Composites Part B-Engineering, 164*, 287–296.

Khan, A., Khan, A. A. P., Asiri, A. M., & Alamry, K. A. (2015). Preparation and Characterization of hybrid graphene oxide composite and its application in paracetamol microbiosensor. *Polymer Composite, 36*, 221–228.

Kinoshita, Y., Wakimoto, K., Gibbons, A. H., Isfahani, A. P., Kusuda, H., Sivaniah, E., et al. (2017). Enhanced PIM-1 membrane gas separation selectivity through efficient dispersion of functionalized POSS fillers. *Journal Membrane Science, 539*, 178–186.

Konnola, R., Nair, C. P. R., & Joseph, K. (2015). Cross-linking of carboxyl-terminated nitrile rubber with polyhedral oligomeric silsesquioxane. *Journal of Thermal Analysis and Calorimetry, 123*, 1479–1489.

Ko, S. W., Hong, M. K., Park, B. J., Gupta, R. K., Choi, H. J., & Bhattacharya, S. N. (2009). Morphological and rheological characterization of multi-walled carbon nanotube/PLA/PBAT blend nanocomposites. *Polymer Bulletin, 63*, 125–134.

Li, C., Li, X., Tao, C., Ren, L., Zhao, Y., Bai, S., et al. (2017). Amphiphilic antifogging/anticing coatings containing POSS-PDMAEMA-b-PSBMA. *ACS Applied Materials & Interfaces, 9*, 22959–22969.

Li, J., Lai, L., Wu, L., Severtson, S. J., & Wang, W.-J. (2018). Enhancement of water vapor barrier properties of biodegradable poly(butylene adipate-co-terephthalate) films with highly oriented organomontmorillonite. *ACS Sustainable Chemistry & Engineering, 6*, 6654–6662.

Li, X., Li, B. H., Lian, S., Dong, X. L., Wang, C. X., & Liang, W. X. (2019). Effects of temperature, moisture and nutrition on conidial germination, survival, colonization and sporulation of Trichothecium roseum. *European Journal of Plant Pathology, 153*, 557–570.

Nakamura, S., & Naka, K. (2013). Size-controlled vaterite composite particles with a POSS-core dendrimer for the fabrication of calcite thin films by phase transition. *Langmuir, 29*, 15888–15897.

Pan, J., Ai, F., Shao, P., Chen, H., & Gao, H. (2019). Development of polyvinyl alcohol/β-cyclodextrin antimicrobial nanofibers for fresh mushroom packaging. *Food Chemistry, 300*, Article 125249.

Tanaka, K., Ishiguro, F., & Chujo, Y. (2010). POSS ionic liquid. *Journal of The Americal Chemical Society, 132*, 17649–17651.

Turan, D., Sängerlaub, S., Stramm, C., & Gunes, G. (2017). Gas permeabilities of polyurethane films for fresh produce packaging: Response of O_2 permeability to temperature and relative humidity. *Polymer Testing, 59*, 237–244.

Waddon, A. J., Zheng, L., Farris, R. J., & Coughlin, E. B. (2002). Nanostructured polyethylene-POSS copolymers: Control of crystallization and aggregation. *Nano Letters, 2*, 1149–1155.

Wu, C., Zhu, Y., Wu, T., Wang, L., Yuan, Y., Chen, J., et al. (2019). Enhanced functional properties of biopolymer film incorporated with curcurmin-loaded mesoporous silica nanoparticles for food packaging. *Food Chemistry, 288*, 139–145.

Wu, Q., Bhattacharya, M., & Morgan, S. E. (2013). POSS-enhanced phase separation in air-processed P3HT:PCBM bulk heterojunction photovoltaic systems. *ACS Applied*

Materials & Interfaces, 5, 6136–6146.
Xie, J., Wang, Z., Zhao, Q., Yang, Y., Xu, J., Waterhouse, G. I. N., et al. (2018). Scale-up fabrication of biodegradable poly(butylene adipate-co-terephthalate)/organophilic-clay nanocomposite films for potential packaging applications. *ACS Omega, 3*, 1187–1196.
Yang, Y. Y., Wang, X., Hu, Y., Hu, H., Wu, D. C., & Xu, F. J. (2014). Bioreducible POSS-cored star-shaped polycation for efficient gene delivery. *ACS Applied Materials & Interfaces, 6*, 1044–1052.
Yun, X., Wang, Y., Li, M., Jin, Y., Han, Y., & Dong, T. (2017). Application of permselective poly(ε-caprolactone) film for equilibrium-modified atmosphere packaging of strawberry in cold storage. *Journal of Food Processing and Preservation, 41*, 13247–13257.
Zhang, J., Zhang, W., & Guan, D. (2015). Preparation and properties of epoxy resin/polyhedral oligomeric silsesquioxane hybrid materials. *Polymer Bulletin, 73*, 113–123.